

# Supporting Information

## **Balancing Robustness, Transparency and Superwetting via Embedding Functional Nanoparticles in V-Groove Architectures**

*Yi Xie<sup>1\*</sup>, Hao Zhang<sup>1</sup>, Xinran Li<sup>1</sup>, Jian Luo<sup>1</sup>, Xiong Qian<sup>2\*</sup>, Yong Zheng<sup>2</sup>, Chuanlin Hu<sup>1</sup>, Ivan P. Parkin<sup>3</sup>, Lee Li<sup>4</sup>, Zhi Chen<sup>5</sup>, Xiujian Zhao<sup>1</sup>*

<sup>1</sup> State Key Laboratory of Silicate Materials for Architectures, Wuhan University of Technology, No. 122, Luoshi Road, Wuhan 430070, P. R. China.

<sup>2</sup> Department of Civil and Environment Engineering, and Research Centre for Resources Engineering towards Carbon Neutrality, The Hong Kong Polytechnic University, Hong Kong, China.

<sup>3</sup> Department of Chemistry, University College London, London WC1H 0AJ, U.K.

<sup>4</sup> State Key Laboratory of Advanced Electromagnetic Engineering and Technology (Huazhong University of Science & Technology), No.1037, Luoyu Road, Wuhan, P. R. China.

<sup>5</sup> Wuhan Shuneng New Material Co., LTD, Wuhan, P. R. China.

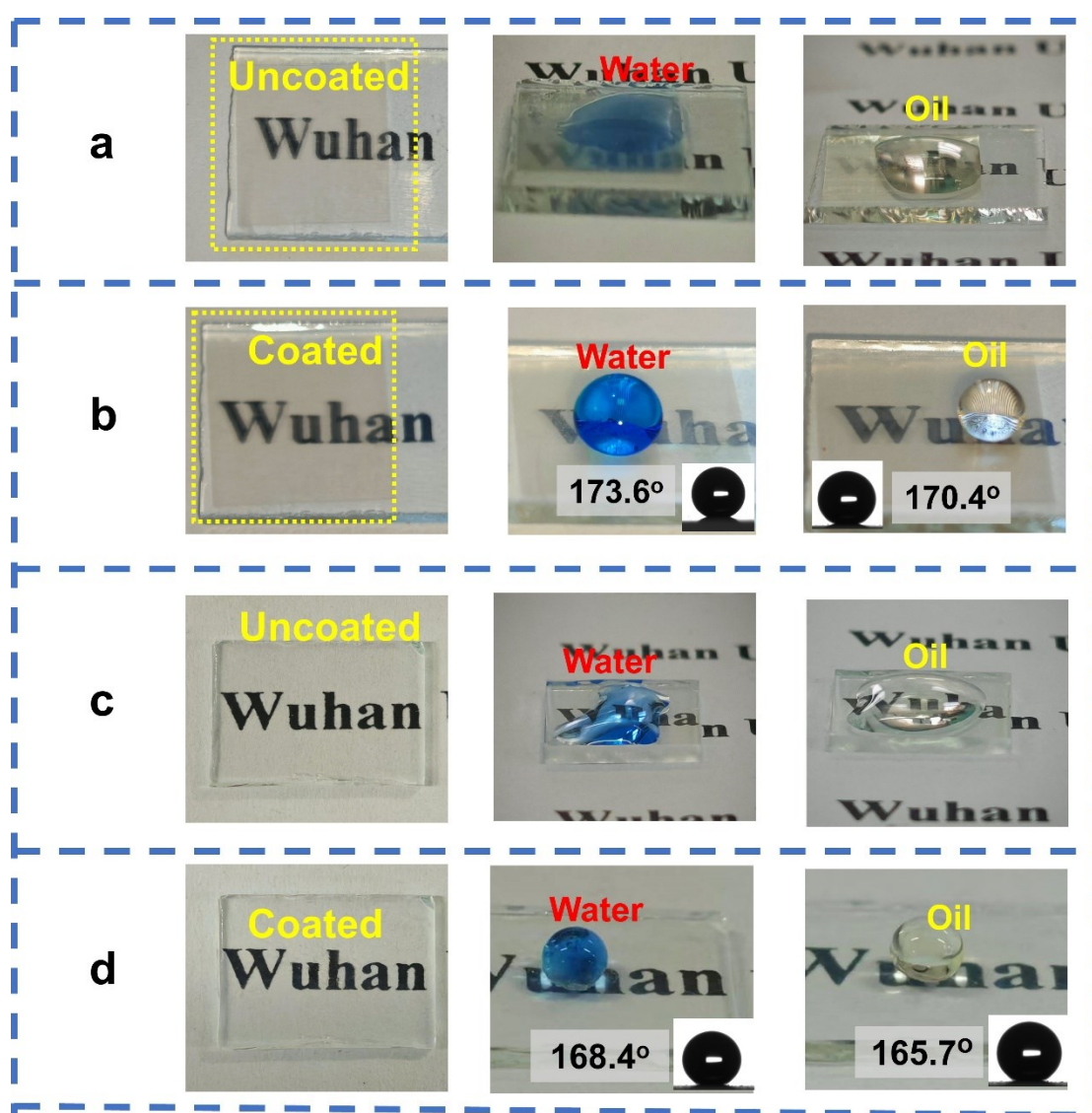


**Figure S1.** Digital photographs of the uncoated laser-etched glass (a), SAP coated laser-etched glass (b), uncoated non-etched glass (c), and the SAP coated non-etched glass (d), together with methylene blue-dyed water and bean oil droplets on each surface to show the surface wettability.

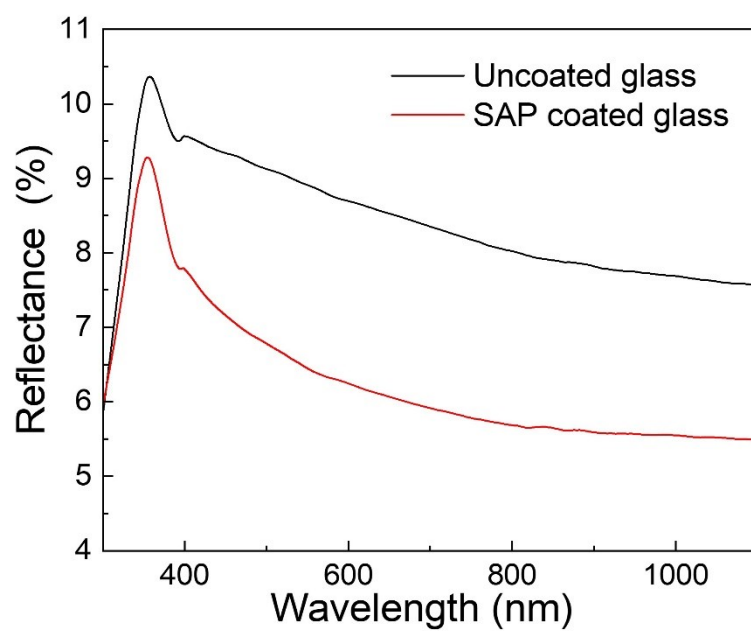


**Figure S2.** Specular reflectance of the bare glass slide and SAP coated glass slide.

**Table S1** Contact angles and sliding angles of various oils on the typical SAP coated laser-etched glass slide

Type of oil	Surface energy (mN·m <sup>-1</sup> )	Contact angles (°)	Sliding angles (°)
Bean oil	31.5	170.1	7.3
Cesame oil	33	171.7	6.4
Corn oil	21.2	161.3	9.0
Pump oil	22	163.8	8.3
n-Hexadecane	27.5	164.2	7.4

**Table S2** Contact angles and sliding angles of various liquids on the typical SAP coated laser-etched glass slide

Type of pollutants	Contact angles (°)	Sliding angles (°)
Coca cola	169.3	3.7
Orange juice	171.2	4.4
Green tea	168.5	3.6
Coconut water	167.3	4.5
Methylene blue solution	170.6	3.9

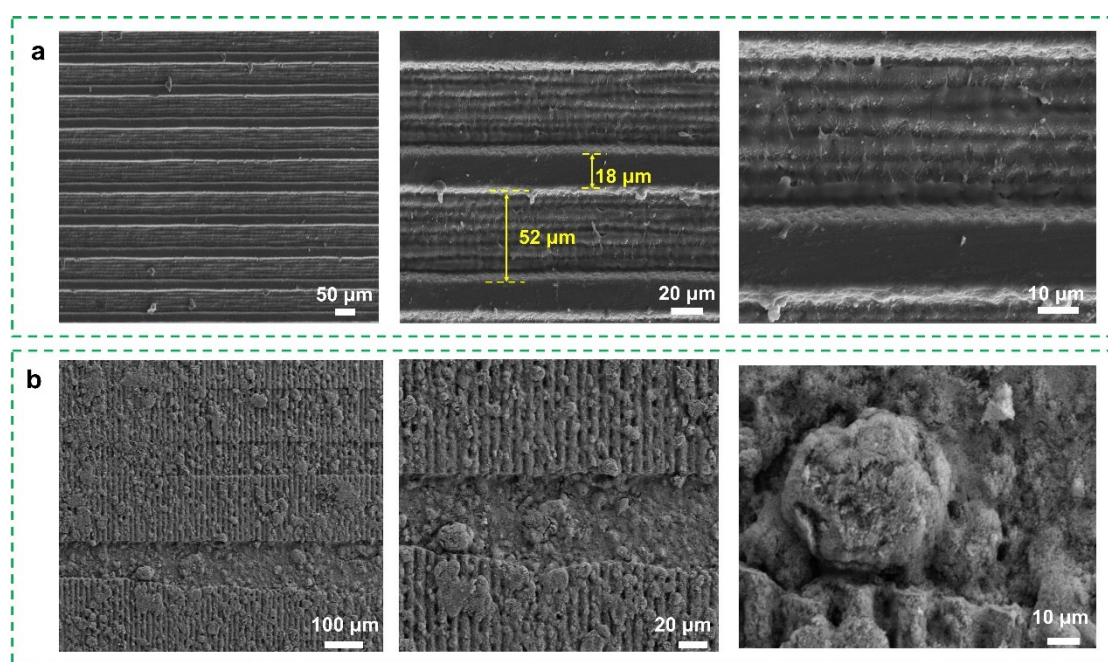


**Figure S3.** Low- and high-magnification SEM images of the uncoated laser-etched glass (a), and the SAP-coated laser-etched glass (b).

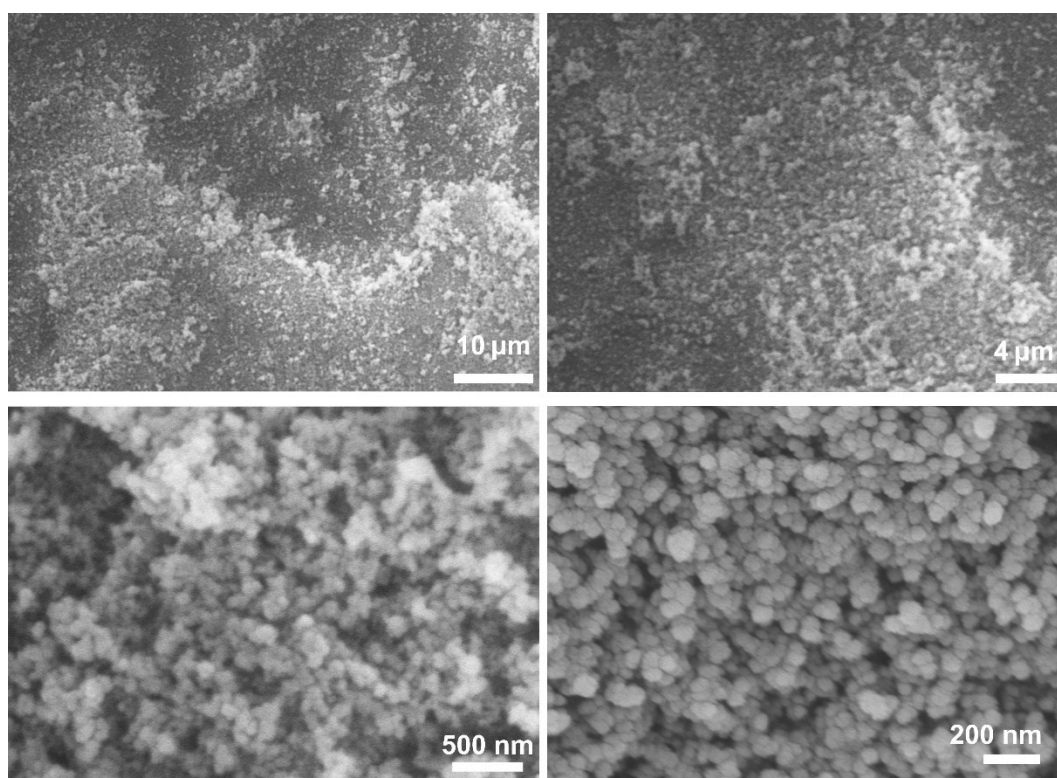


**Figure S4.** Low- and high-magnification SEM images of the SAP coating deposited on non-etched glass.

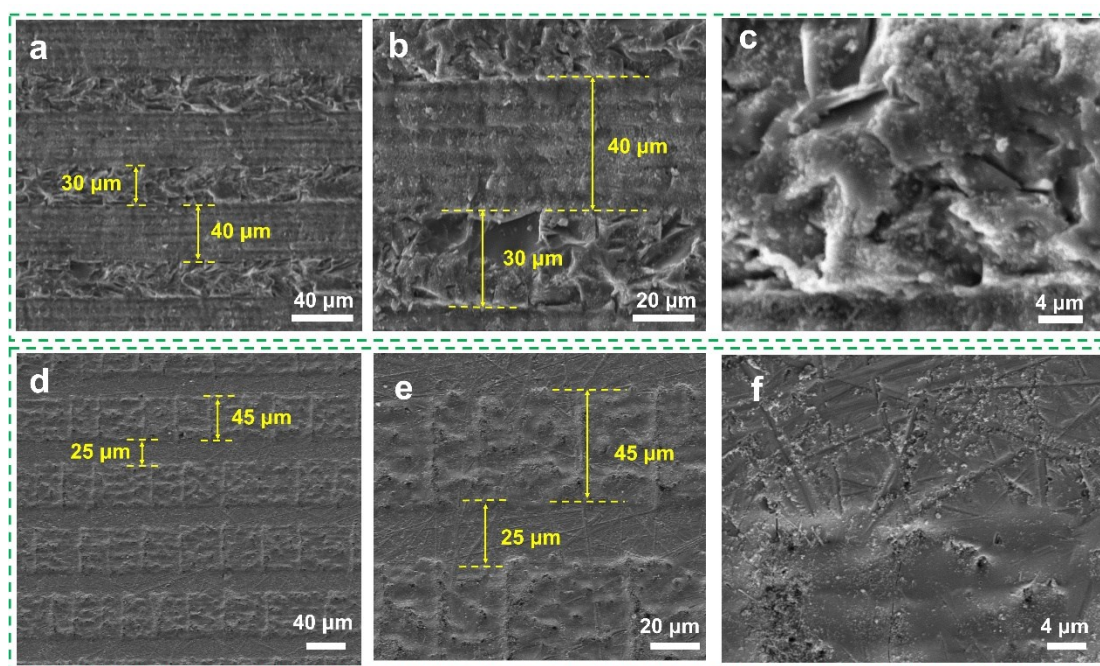


**Figure S5.** Low- and high-magnification SEM images of the SAP-coated laser-etched glass after 50 (a-c) and 100 (d-f) cycles of the abrasion test.



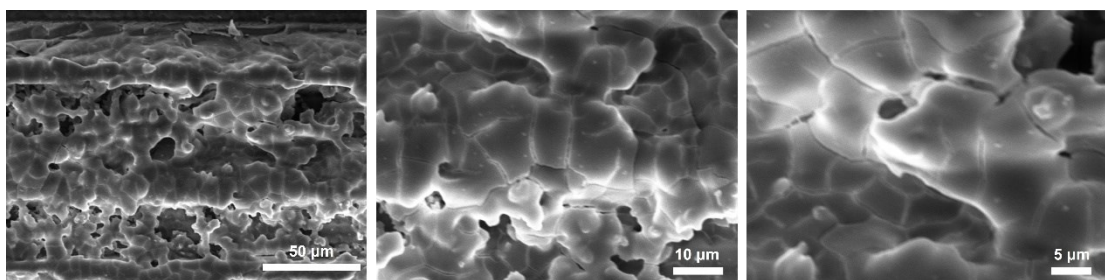


**Figure S6.** SEM image of the as-fabricated SH coated laser-etched sample.



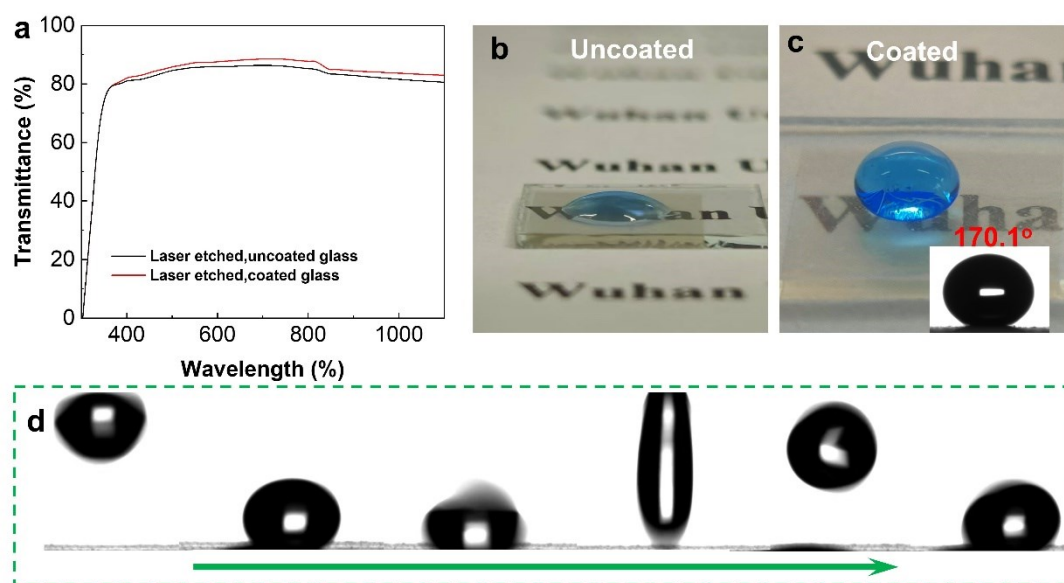


**Figure S7.** (a) Transmittance comparison between laser-etched coated and uncoated glass. (b-c) Digital photographs of the uncoated and SH-coated laser-etched glass, together with water droplets on the surfaces. (d) Selected time-dependent pictures showing water droplet (5  $\mu$ L in volume) impacting and rebounding on the SH surface.

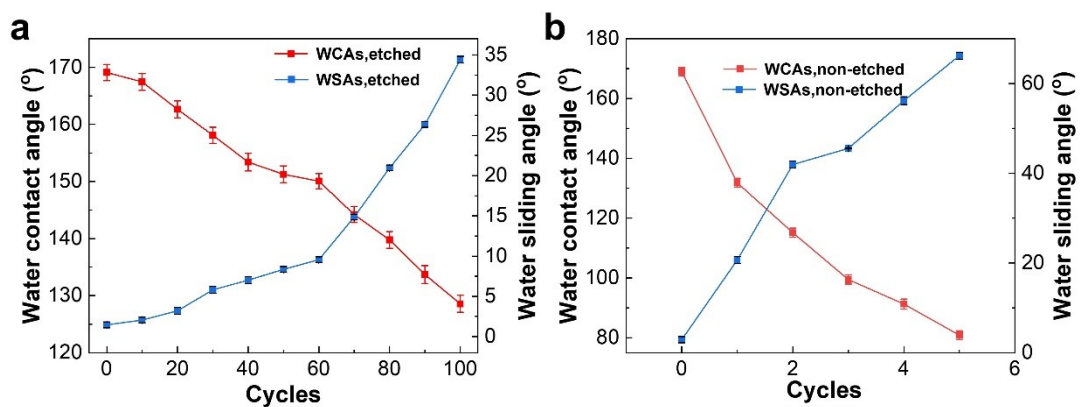


**Figure S8.** WCAs and WSAs vs. sandpaper friction cycles for SH coated laser-etched sample (a) and non-etched sample (b).

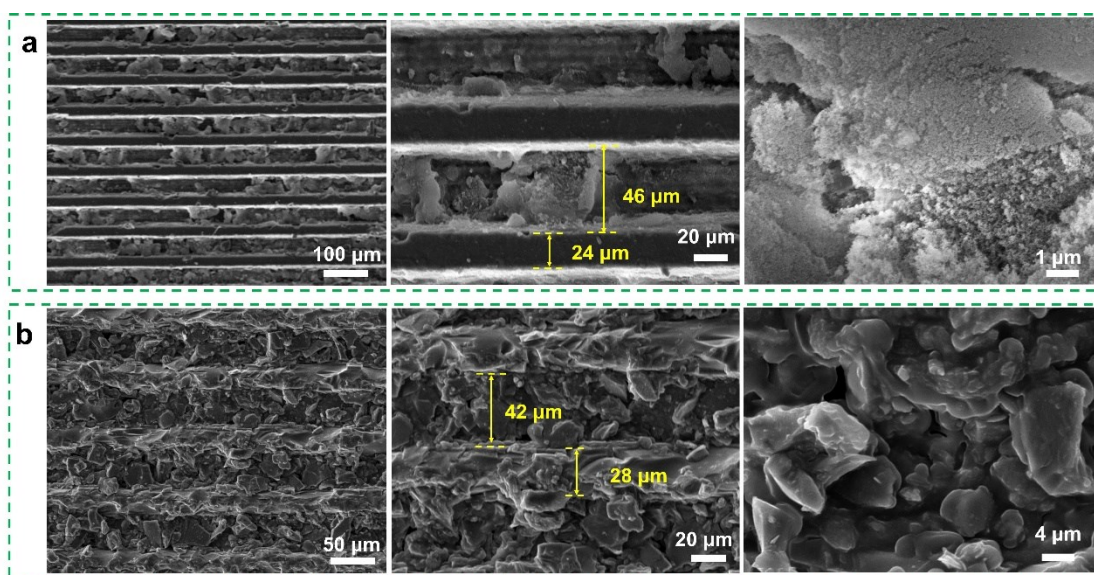


**Figure S9.** Low- and high-magnification SEM images of the SH coated laser-etched glass surface after 50 (a) and 100 (b) sandpaper friction cycles, respectively.

**Table S3.** The comparison of the wear resistance of several superhydrophobic structures obtained by different approaches.

No.	Research	Preparation method	Abrasive paper	Gravity	Area	Pressure	$L_w$
1	Ref. <sup>[1]</sup>	Nanosecond laser	800 #	0.98 N	$1.0 \times 10^{-2} \text{ m}^2$	0.098 kPa	4000 mm
2	Ref. <sup>[2]</sup>	HVOF spraying	800 #	55 N	$2.75 \times 10^{-3} \text{ m}^2$	20 kPa	4800 mm
3	Ref. <sup>[3]</sup>	Laser and the subsequent anodizing	600 #	0.98 N	$2.5 \times 10^{-4} \text{ m}^2$	3.9 kPa	2000 mm
4	Ref. <sup>[4]</sup>	Electrodeposition	1000 #	1.96 N	$1.2 \times 10^{-3} \text{ m}^2$	1.63 kPa	5000 mm
5	Ref. <sup>[5]</sup>	WEDM +laser +heat treatment	600 #	0.98 N	$3.9 \times 10^{-4} \text{ m}^2$	2.5 kPa	5000 mm
6	Ref. <sup>[6]</sup>	Template-assisted spray coating	2000 #	0.49 N	$1.88 \times 10^{-3} \text{ m}^2$	0.26 kPa	1000 mm
7	Ref. <sup>[7]</sup>	Functional SiO <sub>2</sub> -deposited PDMS interlayer	150 #	0.49 N	$1.88 \times 10^{-3} \text{ m}^2$	0.26 kPa	1800 mm
8	Ref. <sup>[8]</sup>	Combining electrodeposition and chemical modification	800 #	0.98 N	$8.1 \times 10^{-4} \text{ m}^2$	1.2 kPa	700 mm
9	Ref. <sup>[9]</sup>	NH <sub>4</sub> OH-assisted sol-gel	600 #	0.98 N	$3.6 \times 10^{-3} \text{ m}^2$	2.7 kPa	2000 mm
10	Our study	Embedding NPs	2000 #	0.49 N	$1.0 \times 10^{-4} \text{ m}^2$	4.9 kPa	5000 mm

		in laser-etched V- groove architecture			m <sup>2</sup>		mm
--	--	--	--	--	----------------	--	----

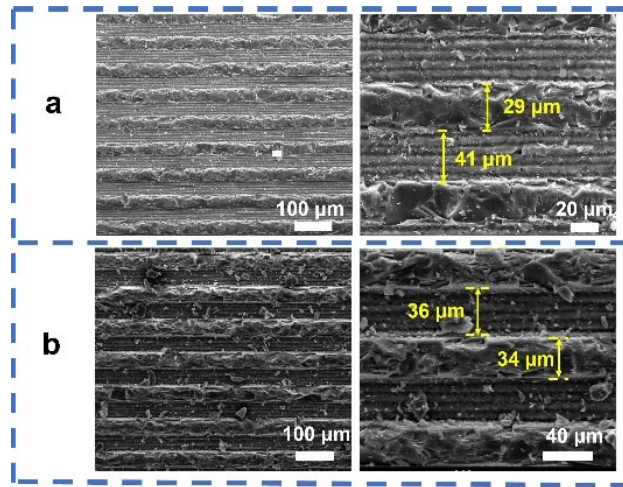


**Figure S10.** SEM images of the uncoated laser-etched glass surface after 50 (a), and 100 (b) cycles of sandpaper abrasion test.

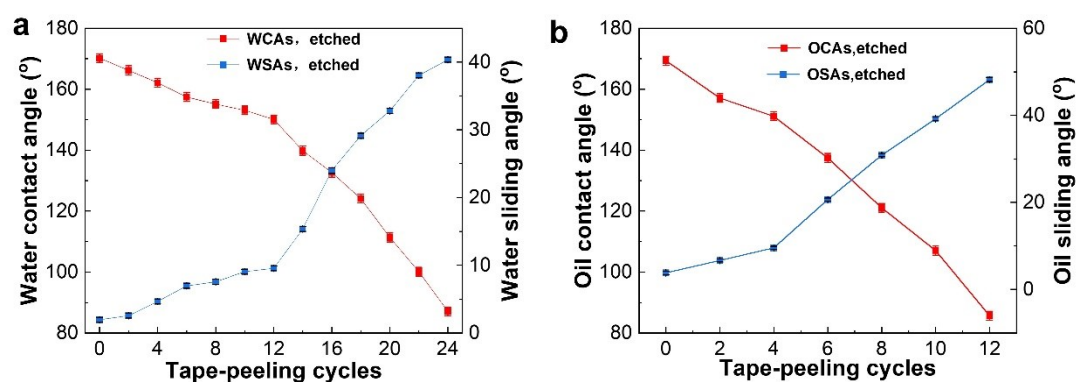


**Figure S11.** Evolution of WCAs/WSAs (a) and OCAs/OSAs over peel-off cycles of tape peeling test performed on SAP coated laser-etched glass slide.



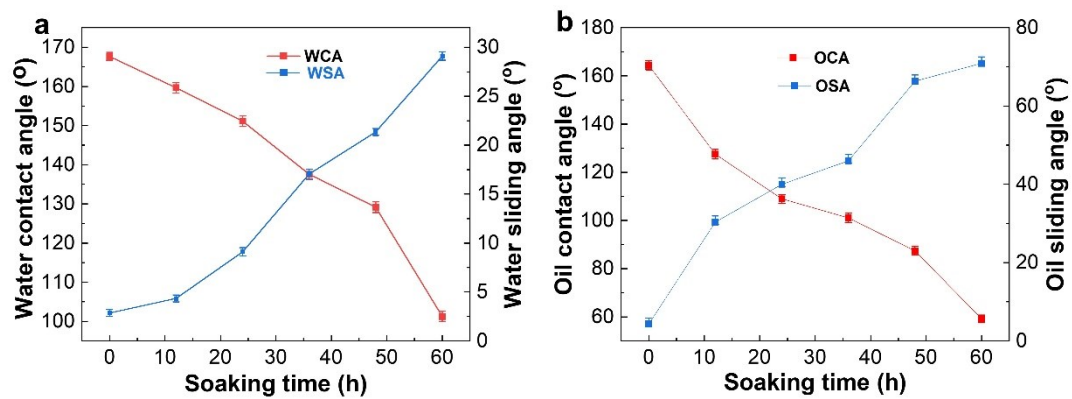


**Figure S12.** Time-dependent WCAs/WSAs (a) and OCAs/OSAs (b) of SAP coating under immersion in NaOH solution with pH value of 13.0.

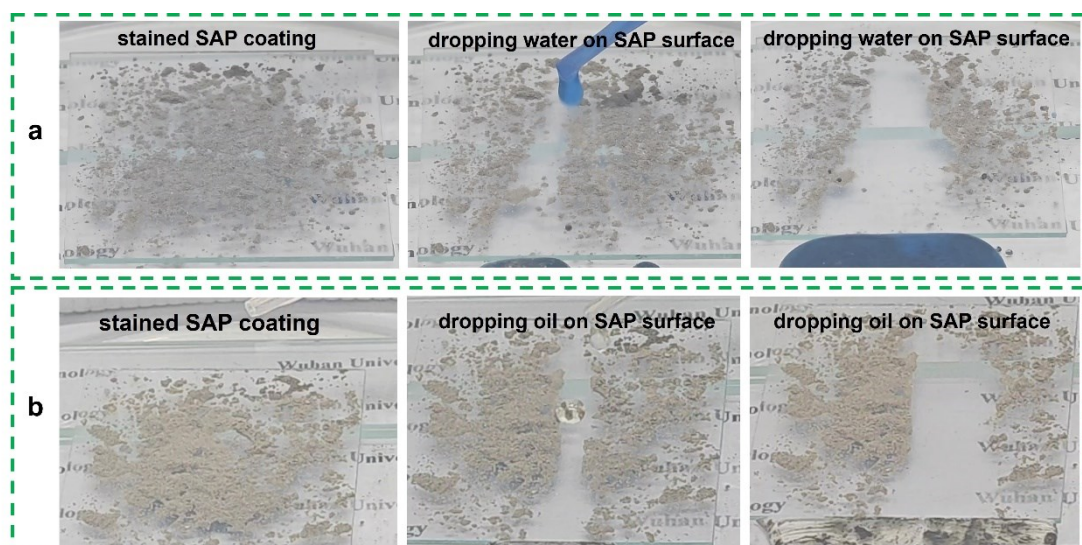


**Figure S13.** Self-cleaning test of the coated laser-etched SAP glass slide. (a) Contamination of the SAP surface by fly-ash, followed by casting methylene blue-dyed water droplets onto the surface to remove the dirt (i.e., fly-ash) and make the surface clean. (b) Contamination of the SAP surface by fly-ash, followed by casting bean oil droplets onto the surface to remove the dirt and make the surface clean.

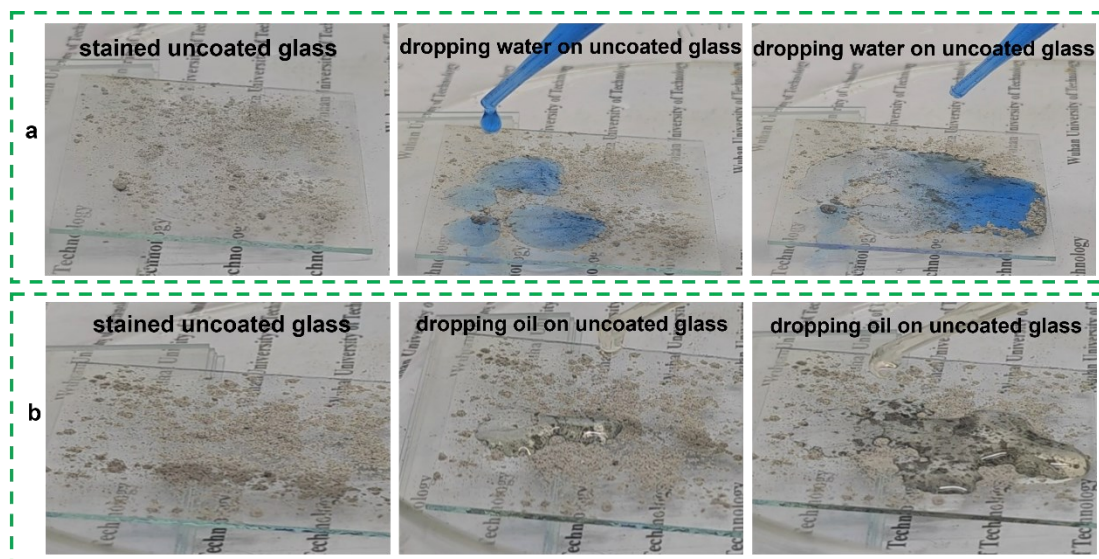


**Figure S14.** Contamination of the uncoated glass slide, followed by dropping water (a) and bean oil (b) onto the glass surface. Both water and pump oil droplets adhere to the uncoated coating, and the surface remains dirty.

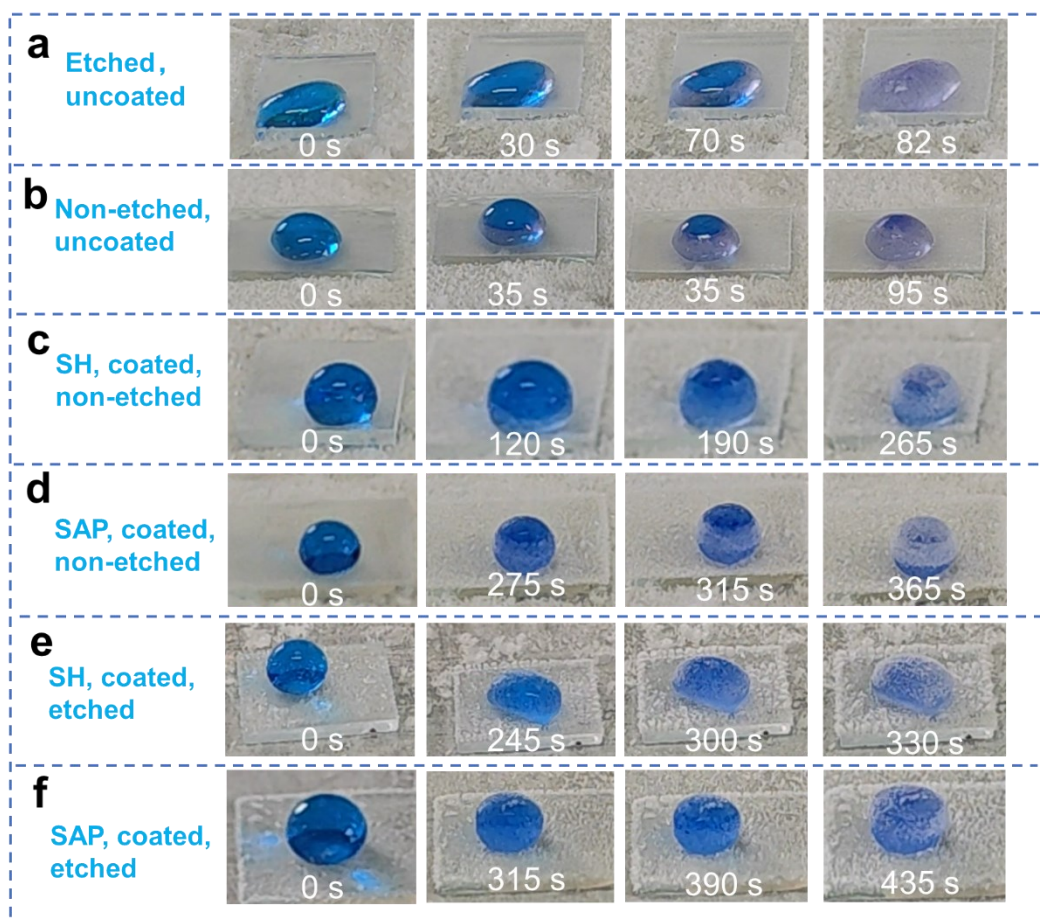


**Figure S15.** Digital photographs of water droplet freezing on uncoated glass slides and various coated samples, demonstrating the freezing time at -10 °C.

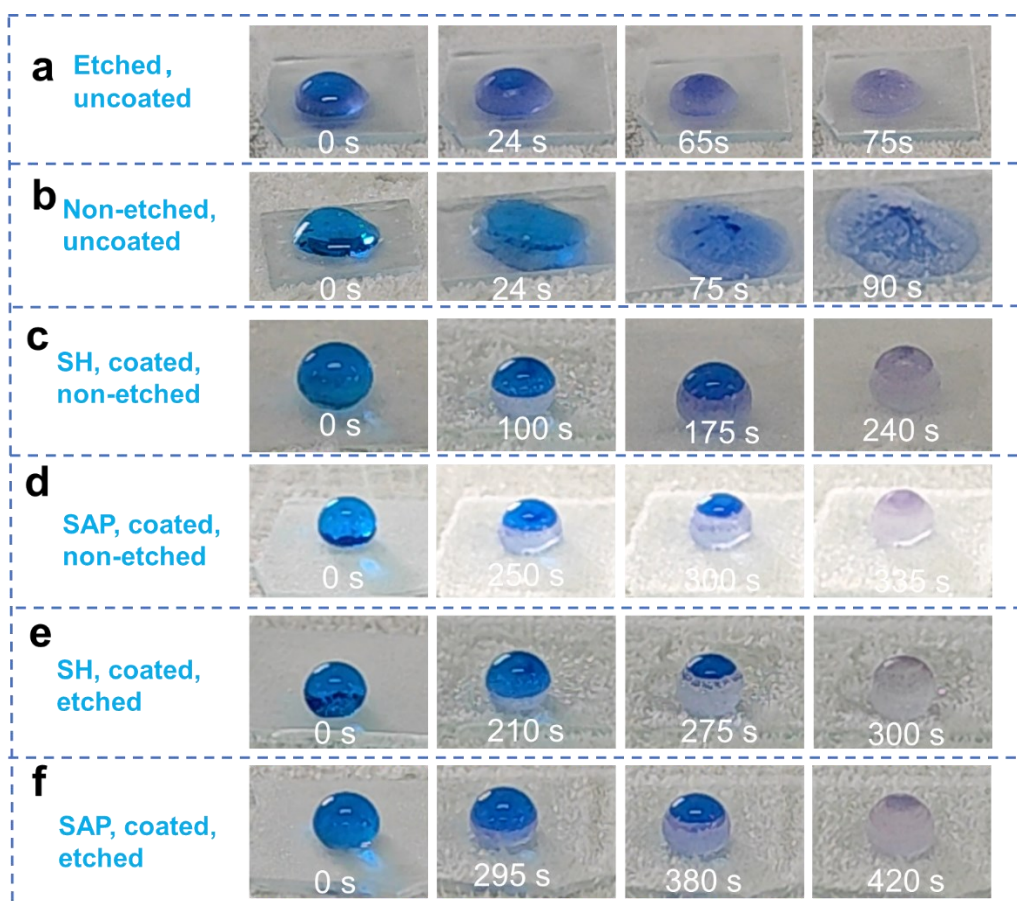


**Figure S16.** Digital photographs of water droplet freezing on uncoated glass slides and various coated samples, demonstrating the freezing time at  $-15\text{ }^{\circ}\text{C}$ .



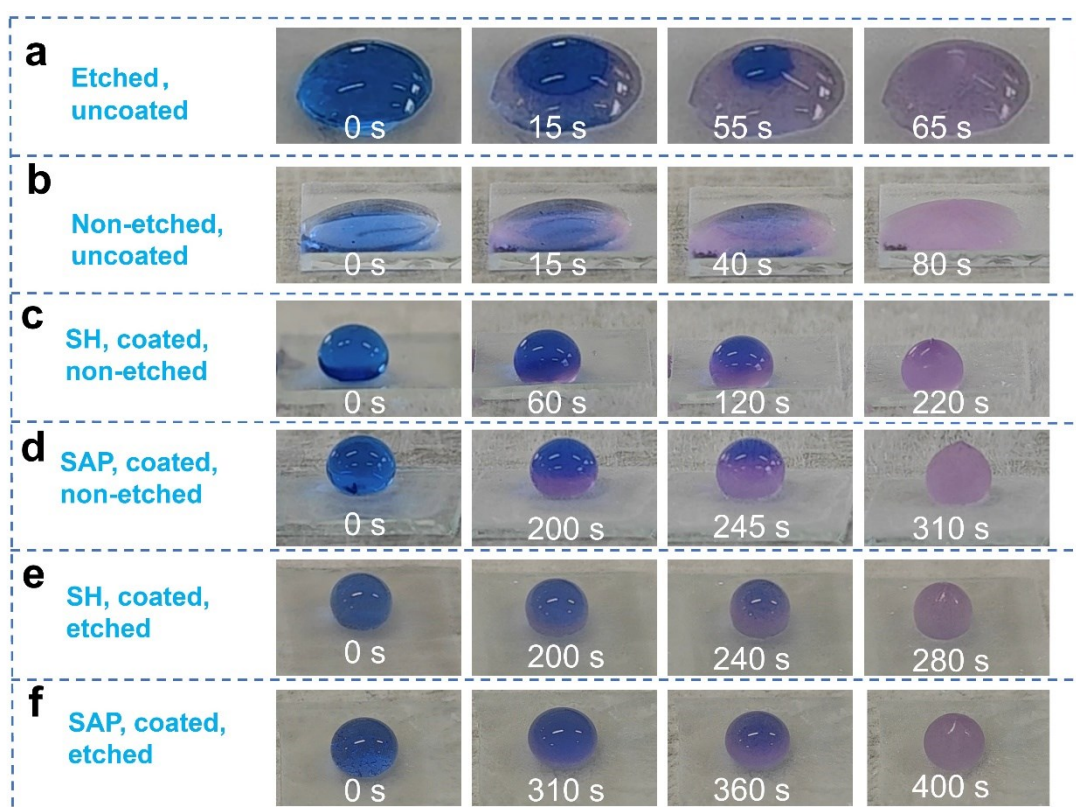


**Figure S17.** Digital photographs of water droplet freezing on uncoated glass slides and various coated samples, demonstrating the freezing time at -20 °C.

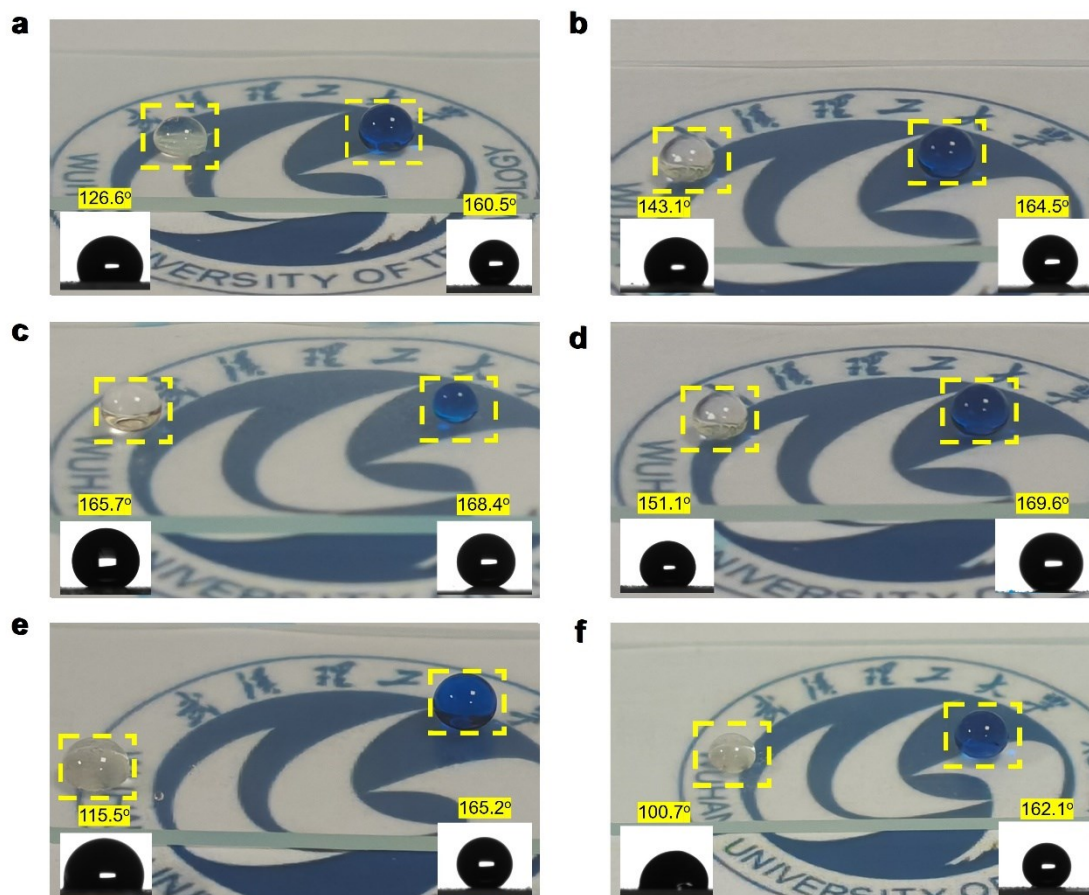


**Figure S18.** Photographic demonstration of transparency and water repellency of the typical coatings deposited on laser-etched glass in the presence of different amounts of NaOH (1.8 M): (a) 0.5 mL, (b) 0.6 mL, (c) 0.7 mL, (d) 0.8 mL, (e) 0.9 mL, and (f) 1.0 mL.



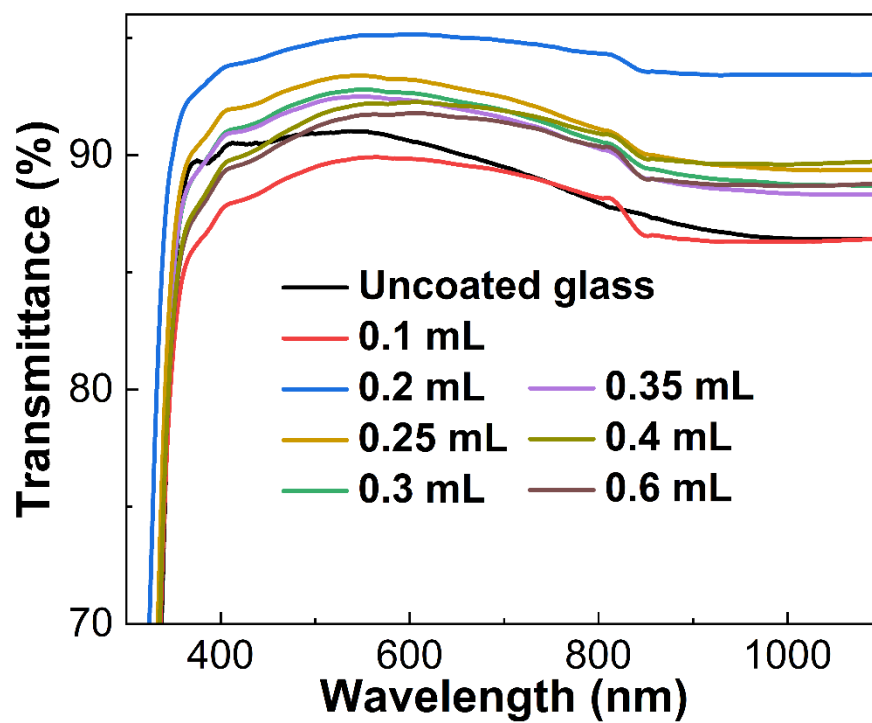


**Figure S19.** Transmittance spectra of the various coatings fabricated in the presence of different NaOH dosages (1.8 M).

## References

1. W. Ren; Z. Lian; J. Wang; J. Xu; H. Yu, "Fabrication of Durable Underoil Superhydrophobic Surfaces with Self-Cleaning and Oil-Water Separation Properties," *Rsc Advances* **2022**, 12 (7), 3838-3846.<https://doi.org/10.1039/d1ra06422c>
2. Y. Liu; N. Xi; S. Fu; G. Yang; H. Fu; H. Chen; X. Zhang; N. Liu; W. Gao, "Mechanical and Chemical Stability of Super-Hydrophobic Coatings on SMA490BW Substrate Prepared by HVOF Spraying," *Materials Research Express* **2018**, 5 (11), 115030.<https://doi.org/10.1088/2053-1591/aadeb3>
3. Y. X. Wang; J. H. Chen; Y. F. Yang; Z. H. Liu; H. Wang; Z. He, "Nanostructured Superhydrophobic Titanium-Based Materials: A Novel Preparation Pathway to Attain Superhydrophobicity on TC4 Alloy," *Nanomaterials* **2022**, 12 (12), 2086.<https://doi.org/10.3390/nano12122086>
4. J. Meng; X. Dong; Y. Zhao; R. Xu; X. Bai; H. Zhou, "Fabrication of A Low Adhesive Superhydrophobic Surface on Ti<sub>6</sub>Al<sub>4</sub>V Alloys Using TiO<sub>2</sub>/Ni Composite Electrodeposition," *Micromachines* **2019**, 10 (2), 121.<https://doi.org/10.3390/mi10020121>
5. Z. Chen; Z. Yang; Z. Zhang; J. Li; G. Zhang; F. Han, "A New Preparation Method of Hierarchical Microstructure for Wear-Resistant Superhydrophobic Surface," *Journal of Materials Research and Technology* **2025**, 36, 4134-4146.<https://doi.org/10.1016/j.jmrt.2025.04.132>
6. H. Li; Q. Jin; H. Li; H. Tong; K. Wang; S. Chen; G. Ouyang; Z. Wang; Y. Li, "Transparent Superamphiphobic Material Formed by Hierarchical Nano Re-Entrant Structure," *Advanced Functional Materials* **2024**, 34 (3), 2309684.<https://doi.org/10.1002/adfm.202309684>
7. P. Wang; M. J. Chen; H. L. Han; X. L. Fan; Q. Liu; J. F. Wang, "Transparent and Abrasion-Resistant Superhydrophobic Coating with Robust Self-Cleaning Function in either Air or Oil," *Journal of Materials Chemistry A* **2016**, 4 (20), 7869-7874.<https://doi.org/10.1039/c6ta01082b>
8. Z. She; Q. Li; Z. Wang; L. Li; F. Chen; J. Zhou, "Researching the Fabrication of Anticorrosion Superhydrophobic Surface on Magnesium Alloy and Its Mechanical Stability and Durability," *Chemical Engineering Journal* **2013**, 228, 415-424.<https://doi.org/10.1016/j.cej.2013.05.017>
9. A. B. Gurav; H. Shi; M. Duan; X. Pang; X. Li, "Highly Transparent, Hot Water and Scratch Resistant, Lubricant-Infused Slippery Surfaces Developed from a Mechanically-Weak Superhydrophobic Coating," *Chemical Engineering Journal* **2021**, 416, 127809.<https://doi.org/10.1016/j.cej.2020.127809>